Physics of Plasmas

Excitation and control of large amplitude standing ion acoustic waves

Cite as: Phys. Plasmas **26**, 092109 (2019); https://doi.org/10.1063/1.5122300
Submitted: 30 July 2019 . Accepted: 04 August 2019 . Published Online: 13 September 2019

L. Friedland, G. Marcus, J. S. Wurtele, and P. Michel

Physics of Plasmas ARTICLE scitation.org/journal/php

Excitation and control of large amplitude standing ion acoustic waves

Cite as: Phys. Plasmas **26**, 092109 (2019); doi: 10.1063/1.5122300
Submitted: 30 July 2019 · Accepted: 4 August 2019 ·
Published Online: 13 September 2019

View Online Export Citation CrossMark

L. Friedland,[1,a)] G. Marcus,[1,b)] J. S. Wurtele,[2,c)] and P. Michel[3,d)]

AFFILIATIONS

[1]Hebrew University of Jerusalem, Jerusalem 91904, Israel
[2]Department of Physics, University of California, Berkeley, California 94720, USA
[3]Lawrence Livermore National Laboratory, Livermore, California 94550, USA

[a)]lazar@mail.huji.ac.il
[b)]gilad.marcus@mail.huji.ac.il
[c)]wurtele@berkeley.edu
[d)]michel7@llnl.gov

ABSTRACT

We study the formation of large-amplitude standing ion acoustic waves (SIAWs) by nonlinear phase-locking (autoresonance) with a weak, chirped frequency standing ponderomotive drive. These waves comprise a nonlinear two-phase solution, with each phase locked to one of the two traveling waves comprising the drive. The autoresonance in the system is guaranteed provided that the driving amplitude exceeds a threshold. The phenomenon is illustrated via water bag simulations within a nonlinear ion fluid model and analyzed using Whitham's averaged variational principle. The local ion and electron densities in the autoresonant SIAWs may significantly exceed the initial unperturbed plasma density and are only limited by kinetic wave-breaking.

I. INTRODUCTION

The interaction of multiple overlapped laser beams with plasmas is relevant to a broad range of problems and applications in optical and plasma sciences. In these situations, the ponderomotive force applied by the beat wave of the overlapped lasers can imprint the refractive structures in the plasma. These structures, whose typical scale is on the order of the light's wavelength, can act like volume gratings and impact the propagation of light in the plasma. This is a situation typically encountered in inertial confinement fusion (ICF), where the overlap of dozens of lasers in the same volume of plasma can lead to complex multiwave coupling problems (for a review, see Ref. 1). Several applications based on light scattering off these optical plasma structures have also been proposed; these include short pulse amplification (long pulse compression) via the resonant excitation of electron or ion-plasma waves,[2–5] transient plasma gratings,[6] crossed-beam energy transfer for symmetry control in ICF,[7] or more recently, plasma-based polarization control.[8–11]

"Plasma photonics," whereby plasmas are used in lieu of solid-state (crystal-based) systems to manipulate the basic properties of light, makes it possible to control and manipulate lasers at fluences many orders of magnitude beyond what solids can sustain. While this research area could be transformative for high-power lasers and all the applications linked to them, its progress is currently challenged by typically poor "energy budgets" in the early experiments: For plasma pulse compression/short pulse amplification, it has been difficult to convert a large fraction of the long pulse "pump" into the short pulse "seed" at relevant intensities. For the plasma polarizer and waveplate concepts, the pump laser used to modify the plasma properties in the initial proof-of-principle experiments used a lot more energy than the "probe" beam whose polarization was being manipulated.[9,10] One of the main reasons for the low efficiency of these schemes is the difficulty to control these plasma structures as they are driven into the nonlinear regime.

In this paper, we explore a new way to drive high amplitude, standing optical plasma structures created by two overlapped pump beams while minimizing the intensity of these pumps. The way to achieve this is by autoresonant excitation of standing ion acoustic waves (SIAWs). Autoresonance is a technique which consists of driving a nonlinear system using a chirped driver slowly sweeping through the linear resonance. Under certain conditions, the nonlinear system can become phase-locked with the driver and will adjust itself to stay in resonance (for a review, see Ref. 12). Autoresonance is a proven

technique for a variety of plasma applications, including the excitation of diocotron modes,[13] nonlinear BGK modes,[14] large amplitude electron plasma waves,[15] and mixing antiprotons with positrons for antihydrogen synthesis.[16] The organization of this paper is as follows: In Sec. II, we present our warm plasma water bag model and illustrate the autoresonant excitation of nonlinear SIAWs in simulations. Section III describes the Lagrangian formulation of the problem. A weakly nonlinear limit of the Lagrangian is used in Sec. IV for calculating the threshold on the driving amplitude for autoresonant excitations using Whitham's averaged variational principle. In Sec. V, we return to fully nonlinear simulations and discuss the tailoring of the driving frequency chirp rate for reaching a quasi-steady state SIAW of a desired amplitude. Finally, Sec. VI summarizes our findings.

II. AUTORESONANT SIAWs IN SIMULATIONS

We proceed by illustrating the excitation of autoresonant SIAWs in numerical simulations. Our model is that of a warm ($T_i/T_e \ll 1$) ion fluid with Boltzmann electrons and the adiabatic ion pressure scaling $p_i \sim n^3$

$$n_t + (nu)_x = 0, \tag{1}$$

$$u_t + uu_x = -\varphi_x - 3u_i^2 n n_x, \tag{2}$$

$$\varphi_{xx} = \exp(\varphi + \varphi_d) - n, \tag{3}$$

where n and u are the ion density and fluid velocity, u_i is the ion thermal velocity, and $\varphi_d = 2\varepsilon \cos\theta_d \cos(kx)$ is a small amplitude ponderomotive driving potential (a standing wave) having a slowly varying frequency $\omega_d(t) = d\theta_d/dt$. Such a drive can be formed by beating two counterpropagating electromagnetic waves having electric fields $E_1 = \tilde{E}_1 \cos(k_0 x - \omega_0 t)$ and $E_2 = \tilde{E}_2 \cos(-k_0 x - \omega_0 t)$, where one of the amplitudes is modulated $\tilde{E}_2 = \bar{E}_2 \cos\theta_d$, with θ_d being the time varying modulation phase. All variables and parameters in our system are dimensionless, such that the time, the position, and the velocities are normalized with respect to the inverse ion plasma frequency $\omega_{pi}^{-1} = (m_i/m_e)^{1/2}\omega_p^{-1}$, the Debye length $\lambda_D = u_e/\omega_p$, and the modified electron thermal velocity $(m_e/m_i)^{1/2}u_e$. The plasma density and the electric potential are normalized with respect to the unperturbed plasma density and $k_B T_e/e$, respectively.

Instead of solving Eqs. (1)–(3) directly, our numerical scheme uses an equivalent water bag model, based on a flat top normalized ion phase space distribution $f(u,x,t) = 1/(2\Delta)$ between two limiting phase space trajectories $u_{1,2}(x,t)$ and vanishing outside these trajectories, with 2Δ being the initial velocity width of the distribution. A similar approach was used recently in studying autoresonant traveling IAWs.[17] The distribution remains constant between and outside the limiting trajectories as they are deformed in the driven problem, and thus, the water bag dynamics is governed by the following momentum and Poisson equations:

$$u_{1t} + u_1 u_{1x} = -\varphi_x, \tag{4}$$

$$u_{2t} + u_2 u_{2x} = -\varphi_x, \tag{5}$$

$$\varphi_{xx} = \exp(\varphi + \varphi_d) - \frac{u_1 - u_2}{2\Delta}. \tag{6}$$

This system transforms into (1)–(3) via $u = (u_1 + u_2)/2$, $n = (u_1 - u_2)/(2\Delta)$, and $\Delta^2 = 3u_i^2$. The advantage of using the water bag model is that it is kinetic and thus yields information on the spread of the trajectories $u_{1,2}$ bounding the ion distribution from the fluid velocity u. This is important in signaling the approach to the kinetic wave breaking limit (see below). Our numerical simulations use the code of Ref. 17 based on a standard spectral method,[18] yielding results illustrated in Figs. 1–3. Panel (a) in Fig. 1 presents the results of the simulations of the water bag system for $\Delta = 0.05$ and linearly chirped driving frequency $\omega_d = \omega_a + \alpha t$, where $\omega_a = k\sqrt{\Delta^2 + 1/(1+k^2)}$ is the linear ion acoustic frequency. We used $k = 0.453$, $\alpha = 10^{-4}$, and $\varepsilon = 0.0044$. The solid line in the figure shows the envelopes of the spatial maxima of the ion fluid velocity u vs slow time $\tau = \sqrt{\alpha}t$. The dotted lines in the same figure illustrate the evolution of the envelopes of the spatial maxima of limiting velocities $u_{1,2}$, while the dashed line is the phase velocity ω_d/k associated with the driving wave. One observes that, after passing the linear resonance, the ion-fluid velocity increases significantly with the upper bound u_1 of the distribution approaching ω_d/k, where one may expect kinetic wave breaking, invalidating our warm fluid approximation. We stop the simulation in this case at $\tau = 4$ to avoid this limit. Panel (b) in Fig. 1 compares the driving frequency ω_d with the excited wave frequency. The latter is evaluated numerically via $\omega = 2\pi/\delta t$, where δt is the time between the successive spatial maxima of u. One can see the efficient frequency locking $\omega \approx \omega_d$ (autoresonance) in the system as the wave amplitude grows continuously beyond the linear resonance. Additional results from the numerical simulation for the parameters of Fig. 1 are presented in Fig. 2, showing the actual spatiotemporal waveform of the electron density $n_e(x,t) \approx \exp\varphi$ during two time intervals of equal duration $\Delta\tau = 0.4$ but starting at different times, $\tau = 0$ [panel (a)] and 3.5 [panel(b)]. One observes the formation of a large amplitude standing wave having a sharply peaked form in panel (b). Finally, Fig. 3 shows the results of the simulations for the same parameters as in Fig. 1, but $\varepsilon = 0.0029$. One can see in panel (a) that the wave excitation saturates shortly after passing the linear resonance as the frequency locking discontinues [see panel (b)]. This effect is associated with the autoresonance threshold phenomenon, where the sustained resonance is expected only when the driving amplitude is above a threshold ε_{th}. In the case of the parameters

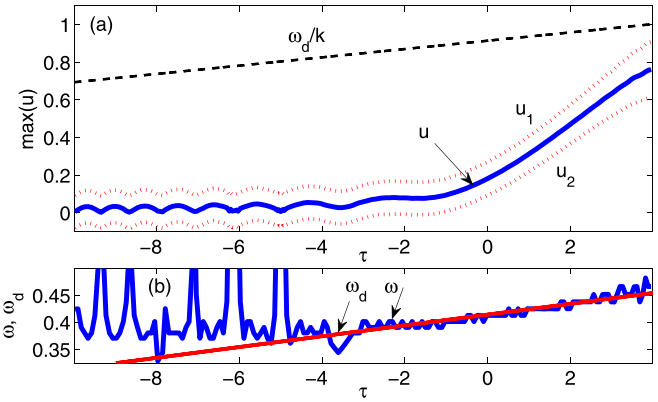

FIG. 1. (a) The ion fluid velocity u vs slow time $\tau = \alpha^{1/2}t$. The solid line represents the envelopes of the maxima of u for $\varepsilon = 0.0044$ (above the threshold $\varepsilon_{th} = 0.0037$). The dotted lines show the envelops of the maxima of velocities $u_{1,2}$ bounding the water bag distribution. The dashed line represents the phase velocity ω_d/k of the driving wave. (b) The frequencies ω_d (in red) and ω (in blue) of the driving and driven waves. One can see the frequency locking (autoresonance) $\omega_d \approx \omega$ beyond $\tau > -4$.

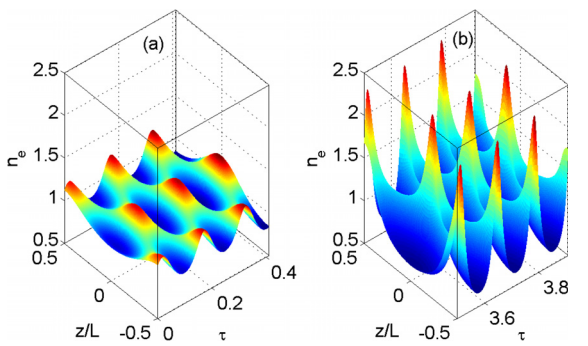

FIG. 2. The wave form of the electron density of the autoresonant SIAW in two time windows of equal duration $\delta\tau = 0.4$ but starting at different times, $\tau = 0$ (at the linear resonance) and $\tau = 3.5$ (near the wavebreaking limit).

used in Fig. 1, the numerically found threshold is $\varepsilon_{th} = 0.0037$. We will discuss this threshold phenomenon in Secs. III and IV with the goal to derive the analytic form of ε_{th} for the chirped frequency excitation of autoresonant SIAWs.

III. LAGRANGIAN COLD ION FLUID LIMIT

For simplifying the theory, here and below we focus on the cold ion fluid limit of (1)–(3), i.e.,

$$n_t + (nu)_x = 0, \tag{7}$$

$$u_t + uu_x = -\varphi_x, \tag{8}$$

$$\varphi_{xx} = \exp(\varphi + \varphi_d) - n. \tag{9}$$

If one starts in the trivial initial state $n = 1$, $u = 0$, $\varphi = 0$, Eqs. (7) and (8) yield, after averaging over one spatial period, the constant-in-time density and fluid velocity $\langle n\rangle = 1$, $\langle u\rangle = 0$. In analyzing driven SIAWs, we discuss the linear stage of excitation first, i.e., we write $n = 1 + \delta n$ and linearize to get

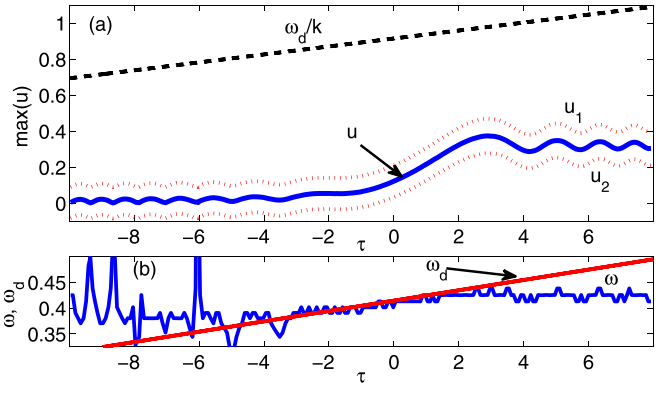

FIG. 3. The ion fluid velocity u vs slow time $\tau = \alpha^{1/2}t$. The thick solid line represents the envelope of the maxima of u for $\varepsilon = 0.0029$ (below the threshold $\varepsilon_{th} = 0.0037$). The dotted lines show the envelopes of the maxima of velocities $u_{1,2}$ bounding the water bag distribution. The dashed line represents the phase velocity ω_d/k associated with the driving wave. (b) The frequencies ω_d and ω of the driving and driven waves, respectively. One can see the frequency locking (autoresonance) $\omega_d \approx \omega$ beyond $\tau = -4$, which discontinues after the passage of the linear resonance.

$$(\delta n)_t + u_x = 0, \tag{10}$$

$$u_t = -\varphi_x, \tag{11}$$

$$\varphi_{xx} = \varphi - \delta n + 2\varepsilon\cos\theta_d\cos(kx). \tag{12}$$

In the case of a constant driving frequency, this set yields a phase-locked standing wave solution of frequency $\omega = \omega_d$

$$\delta n = a\cos(\omega t)\cos(kx), \tag{13}$$

$$u = b\sin(\omega t)\sin(kx), \tag{14}$$

$$\varphi = c\cos(\omega t)\cos(kx), \tag{15}$$

where

$$a = \frac{2\varepsilon k^2}{k^2 - \omega^2(1+k^2)}, \tag{16}$$

$$b = \frac{\omega}{k}a, \tag{17}$$

$$c = \frac{\omega^2}{k^2}a. \tag{18}$$

Our next goal is to generalize this solution to the case of slowly varying driving frequency and include the nonlinearity in the problem. We have seen in simulations the excitation of a slowly varying continuously phase locked (autoresonant) SIAW. This slowness of the excitation process suggests a theoretical approach based on Whitham's averaged variational principle. To this end, we introduce auxiliary potentials ψ and σ, such that $u = \psi_x$, $n = 1 + \sigma_x$, thus transforming Eqs. (7)–(9) into

$$\sigma_{xt} + \left[(1+\sigma_x)\psi_x\right]_x = 0, \tag{19}$$

$$\psi_{xt} + \psi_x\psi_{xx} = -\varphi_x, \tag{20}$$

$$\varphi_{xx} \approx (1+\varphi_d)e^{\varphi} - \sigma_x - 1. \tag{21}$$

This system satisfies a variational principle $\delta(\int L dx dt) = 0$, where the Lagrangian density for the three potentials (σ, ψ, φ) is

$$L = \frac{1}{2}\varphi_x^2 + e^{\varphi+\varphi_d} - \frac{1}{2}(\psi_t\sigma_x + \psi_x\sigma_t) - \left(\frac{1}{2}\psi_x^2 + \varphi\right)n. \tag{22}$$

Since typically the autoresonance threshold is a weakly nonlinear phenomenon,[19] we focus on the weakly nonlinear limit of the problem in Sec. IV, i.e., use

$$L = \frac{1}{2}\varphi_x^2 + V(\varphi) - \frac{1}{2}(\psi_t\sigma_x + \psi_x\sigma_t) - \left(\frac{1}{2}\psi_x^2 + \varphi\right)n + \varphi_d\varphi, \tag{23}$$

where we expanded the electron density $n_e = e^{\varphi+\varphi_d} \approx 1 + \varphi_d + \varphi\varphi_d + \left(\varphi + \frac{1}{2}\varphi^2 + \frac{1}{6}\varphi^3 + \frac{1}{24}\varphi^4\right) = 1 + \varphi_d + \varphi\varphi_d + V(\varphi)$ to the 4th order in φ, neglected $1 + \varphi_d(t)$ in L as not contributing the dynamic, and kept the driving contribution $\varphi\varphi_d$ only, assuming a sufficiently small drive.

IV. WHITHAM'S AVERAGED VARIATIONAL PRINCIPLE

A. Weakly nonlinear ansatz

In studying weakly nonlinear autoresonant SIAWs, we apply Whitham's averaged variational approach.[20] Similar to the autoresonant traveling IAWs,[17] the recipe is to proceed from an ansatz of the

solution to second order in the wave amplitude, substitute this ansatz into the Lagrangian density (23), fix the frequency of both the driver and of the excited wave at some time, and average the Lagrangian density over one spatial and one temporal period (fast scales) associated with the driving wave. This will result in a new averaged Lagrangian density, which depends on slow variables only (i.e., the amplitudes of various harmonics and the phase mismatch in the problem). However, what is the proper second order ansatz for the autoresonant SIAWs? In contrast to the case of traveling waves, where this ansatz is obtained trivially using the solution of the linear problem,[20] finding the nonlinear ansatz for autoresonant SIAWs is more complicated and can be completed as follows: First, we use the spatial periodicity in the problem and write a truncated Fourier expansion of the solutions

$$\begin{aligned}\sigma &= A_1 \sin(kx) + A_2 \sin(2kx),\\ \psi &= B_1 \cos(kx) + B_2 \cos(2kx),\\ \varphi &= C_0 + C_1 \cos(kx) + C_2 \cos(2kx),\end{aligned} \tag{24}$$

where amplitudes A_1, B_1, and C_1 are viewed as small (first order), while A_2, B_2, and $C_{0,2}$ are of second order. Note that spatial averages of σ and ψ vanish, consistent with the initial conditions. The time dependence of the first order amplitudes is assumed to be that of the linear solutions (13)–(15), i.e., $A_1 = (a/k)\cos(\omega t)$, $B_1 = -(b/k)\sin(\omega t)$, and $C_1 = c\cos(\omega t)$. However, what is the time dependence of the second order amplitudes? This problem can be solved by substituting solutions (24) into the Lagrangian density (23) without the driving term and averaging it over one spatial period $2\pi/k$. This yields (via Ref. 21) the averaged Lagrangian density $\bar{\Lambda} = \bar{\Lambda}_2 + \bar{\Lambda}_4$ for solving the time dependent problem, which includes the second and fourth order terms

$$\bar{\Lambda}_2 = \frac{1}{4}\left[C_1^2 + k(A_{1t}B_1 - A_1B_{1t} - 2A_1C_1) + k^2(C_1^2 - B_1^2)\right], \tag{25}$$

$$\begin{aligned}\bar{\Lambda}_4 = {} & \frac{k}{2}(A_{2t}B_2 - A_2B_{2t}) + \frac{1}{2}C_0^2 + \frac{1}{64}(C_1^2 + 4C_2)^2\\ & + \frac{1}{4}C_0C_1^2 - kA_2C_2 + \frac{k^3}{4}B_1(A_2B_1 - 2A_1B_2)\\ & + k^2(C_2^2 - B_2^2).\end{aligned} \tag{26}$$

By using $\bar{\Lambda}$ and taking the variations with respect to A_0, A_2, B_2, and C_2, we obtain the following set of equations:

$$C_0 = -\frac{1}{4}C_1^2, \tag{27}$$

$$B_{2t} = -C_2 + \frac{k^2}{4}B_1^2, \tag{28}$$

$$A_{2t} = 2kB_2 + \frac{k^2}{2}A_1B_1, \tag{29}$$

$$C_2 = \frac{2kA_2}{1+4k^2} - \frac{C_1^2}{4(1+4k^2)}. \tag{30}$$

Equation (27) yields $C_0 \sim \cos^2(\omega t)$ in our ansatz (24) for φ. By the substitution of C_2 from Eq. (30) into (28) and using $C_1^2 \sim \cos^2(\omega t)$, $B_1^2 \sim \sin^2(\omega t)$, we find

$$B_{2t} = -\frac{2kA_2}{1+4k^2} + p\cos^2(\omega t) + r, \tag{31}$$

where p and r are constants, while, similarly, Eq. (29) yields

$$A_{2t} = 2kB_2 + q\sin(2\omega t), \tag{32}$$

where q is constant. The last two equations have the following time periodic solutions:

$$B_2 = b_2 \sin(2\omega t), \tag{33}$$

$$A_2 = A + a_2 \cos(2\omega t), \tag{34}$$

where A, a_2, b_2 are constants. Then, Eq. (30) yields

$$C_2 = C + c_2 \cos(2\omega t), \tag{35}$$

with constant C, c_2. This completes the derivation of the weakly nonlinear ansatz [see Eq. (24)] for the driven SIAWs to be used in Whitham's averaging

$$\begin{aligned}\sigma &= a_1 \cos\theta \sin(kx) + [A + a_2\cos(2\theta)]\sin(2kx),\\ \psi &= b_1 \sin\theta \cos(kx) + b_2 \sin(2\theta)\cos(2kx),\\ \varphi &= c_0 \cos^2\theta + c_1 \cos\theta \cos(kx) + [C + c_2\cos(2\theta)]\cos(2kx),\end{aligned} \tag{36}$$

where we replaced ωt with the wave phase $\theta = \int \omega(t)dt$, assuming a slowly varying frequency of the driven wave. Here, all the amplitudes $a_1, A, a_2, b_1, b_2, c_0, c_1, C, c_2$ are viewed as slow functions of time. The evaluation of these functions and of the wave phase θ in our driven-chirped problem will be discussed in Sec. IV B.

B. Slow evolution system for driven SIAWs

At this stage, we write the driving term in Lagrangian (23) as $\varphi_d = 2\varepsilon\cos(\theta + \Phi)\cos(kx)$, where, assuming a continuing phase-locking (autoresonance) in the system, $\Phi(t)$ is a slow phase mismatch in the problem. Then, following Whitham's recipe, we fix the slow time, substitute ansatz (36) into the Lagrangian density, and average it over one period in space and time. This yields (via Ref. 21) the averaged Lagrangian density $\Lambda = \Lambda_2 + \Lambda_4 + \Lambda_d$, which describes the dynamics of our driven-chirped, weakly nonlinear SIAW. Here

$$\Lambda_2 = \frac{1}{8}\left[c_1^2 - 2ka_1c_1 - k^2(b_1^2 - c_1^2) - 2k\omega a_1b_1\right],$$

$$\begin{aligned}\Lambda_4 = {} & \frac{3}{16}c_0^2 + \frac{3}{32}c_0c_1^2 + \frac{3}{512}c_1^4 + \frac{1}{32}c_1^2c_2 + \frac{1}{8}c_2^2\\ & + \frac{1}{16}Cc_1^2 + \frac{1}{4}C^2 - kAC - \frac{k^2}{2}(b_2^2 - c_2^2 - 2C^2)\\ & - \frac{k^3}{8}b_1\left(\frac{1}{2}a_2b_1 - Ab_1 + a_1b_2\right) - k\omega a_2b_2 - \frac{k}{2}a_2c_2,\end{aligned}$$

$$\Lambda_d = \frac{\varepsilon}{2}c_1\cos\Phi.$$

Note that Λ depends on all slow amplitudes in the problem, as well as on θ via slow frequency $\omega = \theta_t$ and slow mismatch $\Phi = \theta_d - \theta$. Taking variations with respect to c_0, a_2, b_2, c_2, A, and C, respectively, yields the algebraic system

$$4c_0 + c_1^2 = 0, \tag{37}$$

$$8c_2 + k^2b_1^2 + 16\omega b_2 = 0, \tag{38}$$

$$8kb_2 + k^2a_1b_1 + 8\omega a_2 = 0, \tag{39}$$

$$\frac{1}{8}c_1^2 + c_2 - 2ka_2 + 4k^2c_2 = 0, \tag{40}$$

$$-4kC+\frac{1}{2}k^3b_1^2=0, \tag{41}$$

$$\frac{1}{4}c_1^2+2C-4kA+8k^2C=0. \tag{42}$$

This system can be solved to give

$$c_0=-\frac{1}{4}c_1^2, \tag{43}$$

$$a_2=-\frac{kc_1^2-k^2(1+4k^2)(kb_1-2\omega a_1)b_1}{16[-k^2+\omega^2(1+4k^2)]}, \tag{44}$$

$$b_2=-\frac{-2k^3a_1b_1-\omega c_1^2+k^2\omega b_1^2(2+4k^2)}{16[-k^2+\omega^2(1+4k^2)]}, \tag{45}$$

$$c_2=-\frac{-k^4b_1^2+2k^3\omega a_1b_1+\omega^2c_1^2}{8[-k^2+\omega^2(1+4k^2)]}, \tag{46}$$

$$A=\frac{c_1^2+k^2b_1^2(1+4k^2)}{16k}, \tag{47}$$

$$C=\frac{k^2b_1^2}{8}. \tag{48}$$

Next, we again use Λ and take variations with respect to a_1, b_1 to get

$$2c_1+k^2b_1b_2+2\omega b_1=0, \tag{49}$$

$$kb_1(2+ka_2-2Ak)+a_1(k^2b_2+2\omega)=0, \tag{50}$$

yielding relations

$$a_1=\frac{2kc_1+kQ-\omega R}{2\omega^2}, \tag{51}$$

$$b_1=-\frac{2c_1+Q}{2\omega}, \tag{52}$$

where $Q=k^2b_1b_2$ and $R=k^2[b_1(a_2-2A)+a_1b_2]$.

The final stage of our developments is using the average Lagrangian density Λ in taking the variation with respect to c_1, resulting in

$$-ka_1+c_1(1+k^2)+\frac{3}{32}c_1^3+c_1\left(\frac{3}{4}c_0+\frac{1}{4}c_2+\frac{1}{2}C\right)+2\varepsilon\cos\Phi=0, \tag{53}$$

while the variation with respect to phase θ of the wave yields $(\partial\Lambda/\partial\omega)_t=\partial\Lambda/\partial\theta=-\partial\Lambda/\partial\Phi$ or to the lowest (second) significant order in the wave amplitude

$$k(a_1b_1)_t=-2\varepsilon c_1\sin\Phi. \tag{54}$$

In the last equation, we substitute the lowest order results $a_1=kc_1/\omega^2$ and $b_1=-c_1/\omega$, obtained by neglecting the third order terms with P and Q in Eqs. (51) and (52), to get

$$c_{1t}\approx-\varepsilon\frac{\omega^3}{k^2}\sin\Phi. \tag{55}$$

Similarly, we use Eqs. (43), (46), (48), (51), and (52) to express all amplitudes in Eq. (53) in terms of c_1, resulting after some algebra in

$$\left[\frac{k^2}{\omega^2}-(1+k^2)\right]c_1=-Nc_1^3+2\varepsilon\cos\Phi, \tag{56}$$

where $N=q/r$ with $q=4k^8+7k^6(1+4k^2)\omega^2-4k^4(1+4k^2+8k^4)\omega^4-k^2(7+16k^2)\omega^6+4(1+3k^2)\omega^8$ and $r=32\omega^6[\omega^2-k^2(1-4\omega^2)]$.

To the lowest (linear and undriven) order, Eq. (56) yields the linear IAW dispersion relation

$$\omega_a=\frac{k}{\sqrt{(1+k^2)}}. \tag{57}$$

Then, by writing $\omega=\omega_a+\Delta\omega$ and expanding around ω_a in Eq. (56), we find

$$\Delta\omega\approx-\frac{\omega^3}{2k^2}\left(-Nc_1^2+\frac{2\varepsilon}{c_1}\cos\Phi\right). \tag{58}$$

Finally, since $\omega=\omega_d+\Phi_t$, and the driving frequency $\omega_d=\omega_a+\alpha t$, we obtain $\Phi_t=\Delta\omega-\alpha t$ or

$$\Phi_t\approx\beta c_1^2-\alpha t-\frac{\varepsilon}{c_1}\frac{\omega^3}{k^2}\cos\Phi, \tag{59}$$

where $\beta=\frac{\omega^3}{2k^2}N$. By replacing ω by ω_a in β, we find (via Ref. 21)

$$\beta=\frac{4+30k^2+45k^4+27k^6}{192k(1+k^2)^{3/2}}. \tag{60}$$

Equations (55) and (59) comprise a complete set of a standard form describing the passage through linear resonance in many autoresonant systems.[19] Then, as in all other isomorphic systems, if one starts below the resonance ($t_{in}<0$) with $c_1\approx0$ and the driving amplitude ε exceeds the threshold

$$\varepsilon_{th}=0.41\frac{\omega_a^3}{k^2}\frac{\alpha^{3/4}}{\sqrt{\beta}}=5.68\frac{\alpha^{3/4}(1+k^2)^{9/4}}{\sqrt{k(4+30k^2+45k^4+27k^6)}}, \tag{61}$$

the driven-chirped system enters the autoresonant regime. In this regime, the phase mismatch Φ remains bounded, and at larger positive times, c_1^2 increases as $c_1^2\approx\alpha t/\beta$ to stay in a continuing resonance with the drive.

V. AUTORESONANT CONTROL OF SIAWs

The above theory was based on a quasi-linear formalism. Nevertheless, all of our simulations show that the autoresonant evolution continues beyond the quasi-linear approximation, and strongly peaked SIAWs are excited in the process of chirped-driven evolution. Furthermore, as in other autoresonant problems, the variation of the driving frequency need not be linear in time but only sufficiently slow. This allows one to efficiently control the excited wave by, for example, slowing the frequency chirp and approaching any target frequency. Since in autoresonance the amplitude of the excited wave is controlled by the driving frequency, one can arrive to some target amplitude of the excited wave. This target wave will remain phase locked and stabilized, as long as the driving wave is turned on. We illustrate this controlled evolution in Fig. 4 using the numerical simulations of Eqs. (7)–(9). Panel (a) in Fig. 4 shows the envelope of the ion fluid velocity maxima vs slow time $\tau=\alpha^{1/2}t$. In these simulations, we used the driving frequency $\omega_d=\omega_a+\alpha t$ for $t<0$ and $\omega_d=\omega_a+\frac{2\Delta\omega}{\pi}arctg(t/T)$ for $t\geq0$, where $T=\frac{2\Delta\omega}{\pi\alpha}$, so the final driving frequency was $\omega_a+\Delta\omega$. In addition, for a smoother entrance into the autoresonant regime, we slowly ramped up the driving amplitude as $\varepsilon=\varepsilon_0[\frac{1}{2}+\frac{1}{\pi}arctg(t/T)]$,

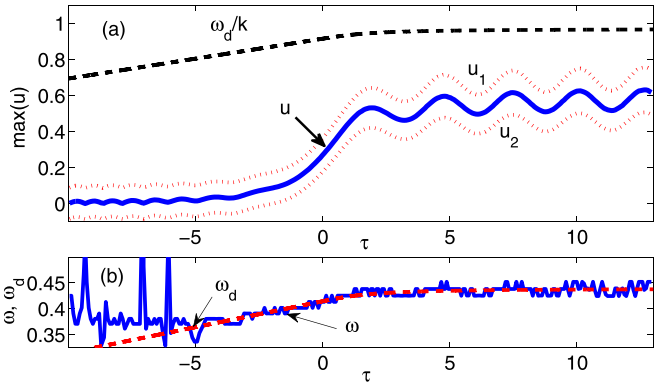

FIG. 4. The autoresonant excitation of a quasi-steady IAW as the driving frequency approaches a constant and the driving amplitude is slowly switched on. (a) The ion fluid velocity u vs slow time $\tau = \alpha^{1/2}t$. The solid line represents the envelopes of the maxima of u. The dotted lines represent the envelopes of the maxima of velocities $u_{1,2}$ bounding the water bag distribution. The dashed line represents the phase velocity ω_d/k associated with the driving wave. (b) The frequencies ω_d and ω of the driving and driven waves, respectively. One can see the continuing frequency locking (autoresonance) $\omega_d \approx \omega$ beyond $\tau > -4$.

and we used parameters $\alpha = 10^{-4}$, $k = 0.453$, $\varepsilon_0 = 0.015$, and $\Delta\omega = 0.025$. The dashed line in the figure shows the phase velocity ω_d/k of the driving wave, while the dotted lines represent the envelopes of velocities $u_{1,2}$ bounding the water bag distribution. One can see in the figure that the fluid velocity maxima saturate as the driving frequency approaches a constant but remain below the wave breaking limit $\max(u) < \omega_d/k$. Panel (b) in Fig. 4 compares the driving frequency ω_d with the excited wave frequency. The latter is evaluated numerically (similar to Figs. 1 and 3) via $\omega = 2\pi/\delta t$, where δt is the time between successive spatial maxima of u. One observes a continuing frequency locking (autoresonance) in the system despite the variation of the driving frequency and amplitude. Finally, Fig. 5 illustrates the actual waveform of the electron density $n_e(x,t)$ of the wave represented in Fig. 4 at the final stage of the excitation ($11 < \tau < 13$). We can see that the excited wave comprises a pattern having a two phase form $u(x,t) = u(\theta_1, \theta_2)$, where the phases are $\theta_{1,2} = \pm kx - \omega t$. One can clearly see in the figure two directions $x/t = \pm\omega/k$ along which one of the

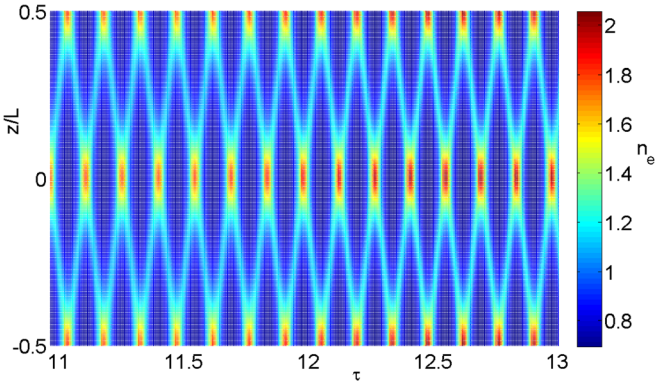

FIG. 5. The colormap of the wave form of the electron density of the standing autoresonant IAW in time window $11 < \tau < 13$ for the example given in Fig. 4.

phases remains constant, and the space-time periodicity of the solution is dictated by the second phase. This result is remarkable since the existence of two phase solutions in nonlinear wave problems is unusual and indicates some integrability in the system. The integrability may be related to the fact that SIAWs having small amplitude and k are described by the KdV equation, which is integrable and admits multiphase solutions.[22]

VI. CONCLUSIONS

We have shown theoretically and numerically that a large amplitude SIAW can be excited and controlled with a small amplitude chirped drive. The analysis of the ion dynamics assumed thermal electrons and a warm ion fluid. The warm ion fluid model was, following the approach in Ref. 17, derived from a water bag Vlasov distribution so that the standard momentum and density equations were replaced by the equations for the upper and lower velocities confining the Vlasov function [Eqs. (4)–(6)].

The theory employed a weakly nonlinear Lagrangian analysis and Whitham's averaging technique to find two differential equations that describe the evolution of the slowly varying amplitude [Eq. (55)] and the phase [Eq. (59)] of the first harmonic of the potential. The slowly varying solutions for the fluid velocity u and density n can be derived from the solution to Eqs. (55) and (59). These equations are in the standard form for an autoresonant system and therefore exhibit a well-known threshold, [Eq. (61)], on the amplitude of the normalized drive potential required for autoresonance.

Fully nonlinear numerical simulations (using the algorithm in Ref. 17) confirm these theoretical predictions. Moreover, they demonstrate that extremely large density perturbations can be created when operating above threshold. The autoresonant nature of the interaction ties the amplitude of the density oscillation to the frequency of the chirped drive. An important result here is that the amplitude of density perturbation can be controlled by appropriate tailoring of the drive frequency evolution so that the chirping stops at some desired frequency. This is seen in Figs. 4 and 5. Finally, the standing wave is seen to correspond to two-phase solutions of the nonlinear system; this may be related to the small amplitude KdV limit of the SIAW equations.

This analysis avoided particle trapping by operating in a regime where the fluid velocity is well below resonance. Further extensions would include a full kinetic simulation to study the interplay of autoresonance and the excitation of BGK-like modes in the ion kinetic distribution. The model assumes that the ponderomotive drive is prescribed, while actual implementation would likely require two laser pulses, one of which needs to have a chirped frequency. The evolution of the coupled three-wave system that describes nonlinear SIAWs requires further investigation.

ACKNOWLEDGMENTS

This work was supported by the NSF-BSF under Grant No. 1803874 (BSF No. 6079) and performed under the auspices of the U.S. DOE by LLNL under Contract No. DE-AC52-07NA27344, with support from the LLNL-LDRD Program under Project Tracking No. 18-ERD-046.

REFERENCES

[1]J. F. Myatt, J. Zhang, R. W. Short, A. V. Maximov, W. Seka, D. H. Froula, D. H. Edgell, D. T. Michel, I. V. Igumenshchev, D. E. Hinkel, P. Michel, and J. D. Moody, Phys. Plasmas **21**, 055501 (2014).
[2]V. M. Malkin, G. Shvets, and N. J. Fisch, Phys. Rev. Lett. **82**, 4448 (1999).
[3]G. Shvets, N. J. Fisch, A. Pukhov, and J. Meyer-ter Vehn, Phys. Rev. Lett. **81**, 4879 (1998).
[4]A. A. Andreev, C. Riconda, V. T. Tikhonchuk, and S. Weber, Phys. Plasmas **13**, 053110 (2006).
[5]L. Lancia, A. Giribono, L. Vassura, M. Chiaramello, C. Riconda, S. Weber, A. Castan, A. Chatelain, A. Frank, T. Gangolf, M. N. Quinn, J. Fuchs, and J.-R. Marqu'es, Phys. Rev. Lett. **116**, 075001 (2016).
[6]G. Lehmann and K. H. Spatschek, Phys. Rev. Lett. **116**, 225002 (2016).
[7]P. Michel, L. Divol, E. A. Williams, S. Weber, C. A. Thomas, D. A. Callahan, S. W. Haan, J. D. Salmonson, S. Dixit, D. E. Hinkel, M. J. Edwards, B. J. MacGowan, J. D. Lindl, S. H. Glenzer, and L. J. Suter, Phys. Rev. Lett. **102**, 025004 (2009).
[8]P. Michel, L. Divol, D. Turnbull, and J. D. Moody, Phys. Rev. Lett. **113**, 205001 (2014).
[9]D. Turnbull, P. Michel, T. Chapman, E. Tubman, B. B. Pollock, C. Y. Chen, C. Goyon, J. S. Ross, L. Divol, N. Woolsey, and J. D. Moody, Phys. Rev. Lett. **116**, 205001 (2016).
[10]D. Turnbull, C. Goyon, G. E. Kemp, B. B. Pollock, D. Mariscal, L. Divol, J. S. Ross, S. Patankar, J. D. Moody, and P. Michel, Phys. Rev. Lett. **118**, 015001 (2017).
[11]G. Lehmann and K. H. Spatschek, Phys. Rev. E **97**, 063201 (2018).
[12]J. Fajans and L. Friedland, Am. J. Phys. **69**, 1096 (2001).
[13]J. Fajans, E. Gilson, and L. Friedland, Phys. Rev. Lett. **82**, 4444 (1999).
[14]L. Friedland, F. Peinetti, W. Bertsche, J. Fajans, and J. Wurtele, Phys. Plasmas **11**, 4305 (2004).
[15]R. R. Lindberg, A. E. Charman, J. S. Wurtele, L. Friedland, and B. A. Shadwick, Phys. Plasmas **13**, 123103 (2006).
[16]C. Amole, M. D. Ashkezari, M. Baquero-Ruiz, W. Bertsche, E. Butler, A. Capra, C. L. Cesar, M. Charlton, A. Deller, S. Eriksson, J. Fajans *et al.*, Phys. Plasmas **20**, 043510 (2013).
[17]L. Friedland and A. G. Shagalov, Phys. Plasmas **24**, 082106 (2017).
[18]C. Canuto, M. Y. Hussaini, A. Quarteroni, and T. A. Zang, *Spectral Methods in Fluid Dynamics* (Springer-Verlag, New York, 1988).
[19]L. Friedland, Scholarpedia **4**, 5473 (2009).
[20]G. B. Whitham, *Linear and Nonlinear Waves* (Wiley, New York, 1974).
[21]Wolfram Research, Inc., Mathematica, Version 11.1, Champaign, IL, 2017.
[22]L. Friedland and A. G. Shagalov, Phys. Rev. Lett. **90**, 074101 (2003).